Medical Engineering & Physics 33 (2011) 1234–1244

Contents lists available at ScienceDirect

Medical Engineering & Physics

journal homepage: www.elsevier.com/locate/medengphy

A new thermal model for bone drilling with applications to orthopaedic surgery

JuEun Lee, Yoed Rabin, O. Burak Ozdoganlar*

Carnegie Mellon University, Department of Mechanical Engineering, Pittsburgh, PA 15213, USA

ARTICLE INFO

Article history:
Received 29 October 2010
Received in revised form 11 April 2011
Accepted 25 May 2011

Keywords:
Bone drilling
Orthopaedic surgery
Osteonecrosis
Thermal model
Heat transfer

ABSTRACT

This paper presents a new thermal model for bone drilling with applications to orthopaedic surgery. The new model combines a unique heat-balance equation for the system of the drill bit and the chip stream, an ordinary heat diffusion equation for the bone, and heat generation at the drill tip, arising from the cutting process and friction. Modeling of the drill bit-chip stream system assumes an axial temperature distribution and a lumped heat capacity effect in the transverse cross-section. The new model is solved numerically using a tailor-made finite-difference scheme for the drill bit-chip stream system, coupled with a classic finite-difference method for the bone. The theoretical investigation addresses the significance of heat transfer between the drill bit and the bone, heat convection from the drill bit to the surroundings, and the effect of the initial temperature of the drill bit on the developing thermal field. Using the new model, a parametric study on the effects of machining conditions and drill-bit geometries on the resulting temperature field in the bone and the drill bit is presented. Results of this study indicate that: (1) the maximum temperature in the bone decreases with increased chip flow; (2) the transient temperature distribution is strongly influenced by the initial temperature; (3) the continued cooling (irrigation) of the drill bit reduces the maximum temperature even when the tip is distant from the cooled portion of the drill bit; and (4) the maximum temperature increases with increasing spindle speed, increasing feed rate, decreasing drill-bit diameter, increasing point angle, and decreasing helix angle. The model is expected to be useful in determination of optimum drilling conditions and drill-bit geometries.

1. Introduction

Heat generation during bone drilling may result in thermal injury due to exposure to elevated temperatures, with potentially devastating effects on the outcome of orthopaedic surgery. Depending on the magnitude of the temperature elevation and the exposure time, heat generation during bone drilling may lead to hyperthermia and even carbonization, resulting in cell death and bone-property changes [1,2]. Similarly, bone resorption may occur due to a sufficient thermal insult and resulting thermonecrosis. During bone drilling, heat is generated mainly from the cutting process (shear deformations) and the friction between the rake face of the drill bit and the chips; secondary heating effects are driven by friction between the chips, drill bit body, and the bone [3]. Moreover, thermal effects during bone drilling may lead to immediate vascular damage, which, in a somewhat longer term, adds to bone death (osteonecrosis) due to insufficient blood supply [4].

Experimental investigations to prevent thermal osteonecrosis by identifying favorable drilling conditions and drill-bit geometries are reported in the literature [5–7]. Although those reports provide a variety of (and sometimes conflicting) conclusions on how to decrease thermal injury during bone drilling, they display a consensus that the level of temperature elevation and the duration of thermal exposure must be minimized.

The heat generation during drilling is directly determined by the drill-bit geometry [8,9]. With reference to Fig. 1, the design of the drill-bit point and the cutting edges dictates the cutting forces for given drilling conditions. A large portion of the energy used for shear deformations and the friction on the rake face is transformed into heat, which is the main heat source during bone drilling. Although a smaller point angle could be preferable to reduce shear deformations (reduced shear stresses), for a given drill-bit diameter, it also makes the cutting edge longer. It follows that a higher point angle may affect heat generation in different ways [2], depending on the complete set of geometric parameters. However, it has been suggested in the literature that the overall effect of point angle is negligibly small [10,11].

The chisel-edge design also has a strong effect on the cutting forces. However, since the chisel edge mainly contributes to the thrust forces, its effect on heat generation is secondary to the effect of the cutting edges. Furthermore, the geometry of the drill-bit

* Corresponding author at: Carnegie Mellon University, Department of Mechanical Engineering, 5000 Forbes Avenue, Pittsburgh, PA 15213, USA.
Tel.: +1 4122689890; fax: +1 4122683348.
E-mail addresses: ozdoganlar@cmu.edu, burakoz@andrew.cmu.edu (O.B. Ozdoganlar).

1350-4533/$ – see front matter © 2011 Published by Elsevier Ltd on behalf of IPEM.
doi:10.1016/j.medengphy.2011.05.014

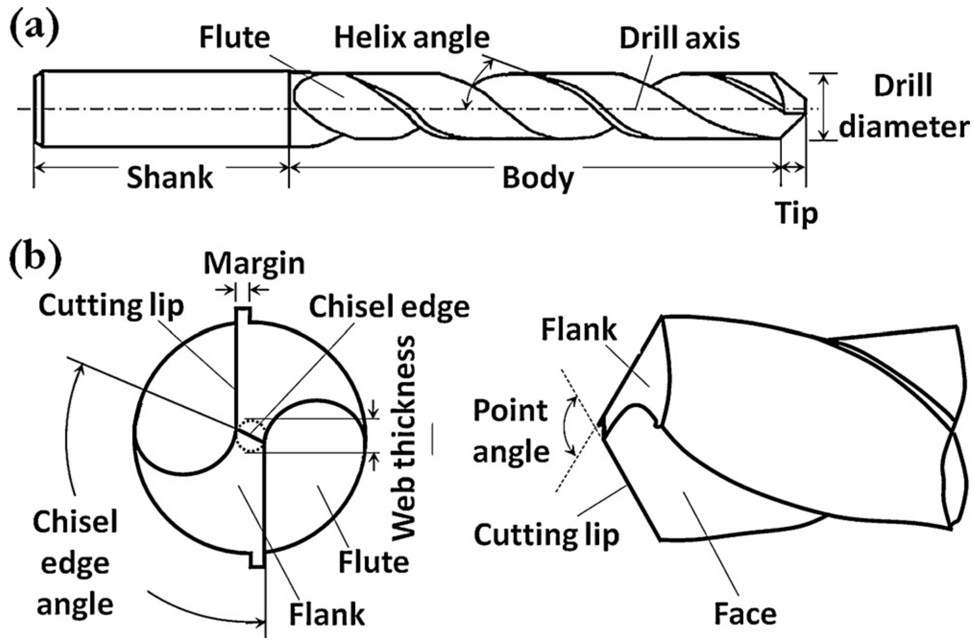

Fig. 1. Drill-bit geometry: (a) twist drill bit and (b) drill-bit tip.

flutes (i.e., the cross-section of the drill-bit body) determines the compaction and speed of the chips expelled from the cutting region [12]. Since the chips absorb a portion of the generated heat, a faster chip stream within the flutes may reduce the overall amount of heat transferred to the bone [8]. A faster chip stream may also lower the maximum temperature in the process, even if the overall heat transfer to the bone is unaffected significantly, which may be typical to a relatively deep drill-bit penetration. Since the helix angle also affects the cutting edge geometry and the fluted region geometry, it also has a considerable effect on the generated temperatures [7].

Since the heat generation increases linearly with the cutting speed, when the other parameters are held constant, increasing the drill-bit diameter increases the amount of heat generation, which results in higher temperatures [5]. From the same reason, increasing the feed rate and, independently, the spindle speed [13] also increases the generated heat. The initial thermal damage, as well as the post-surgery bone healing, has shown to be affected by the spindle speeds, where higher speed intensified the thermal damage and extended the healing time [14].

In certain cases, the competing effects of higher local heat generation and reduced heat transfer to the bone may cancel one another, resulting in heat generation independent of the cutting speeds [15]. Although one could assume that lower feed rate and slower spindle speed are always favorable in reducing thermal effects, based on the above discussion, other effects may play competing roles, and especially during drilling of a low conductivity material, such as bone. This may explain why, in many cases, the bone temperatures were found to be lower at higher feed rates when drilling different bone sections [10,13]. Being highly conductive compared with bone, the drill bit can actually cool the cutting edge by heat conduction, and especially when externally cooled. The chip stream itself convects heat from the cutting edge, along the flute, creating a cooling mechanism, where a higher feed rate leads to a faster chip stream, with higher cooling capabilities. Here, for example, the higher feed rate represents a competing effect between higher heat generation due to faster cutting and a higher cooling effect due to heat convection by the chip stream. Indeed, it has been reported in the literature that higher spindle speeds may result in lower temperatures and reduced thermal injury in bone drilling [16,17] and oral surgery [20–22].

The complex relationships between the drill-bit geometry, chip stream, drilling conditions, and bone characteristics pose a great challenge in determining the favorable and, ultimately, optimal set of bone drilling parameters to minimize thermal effects. Moreover, the large number of significant drilling parameters makes the study and optimization of the bone drilling through experiments alone impractical. To the best of our knowledge, only a few attempts have been made to develop a thermal model for the bone drilling process. Davidson and James [23] suggested a thermal model to predict temperature elevation in bone during drilling. In their model, the conduction equation was solved in a two-dimensional domain using Galerkin's finite-element method. However, they only considered heat generation at the drill-bit tip, while neglecting the significant effects of moving chips, heat transfer between the drill-bit body and the bone, and heat convection from the drill bit to the surroundings outside the bone. Kalidindi [24] performed an analytical study to predict the temperature distribution during dental drilling for implant surgery. A homogenous differential equation of heat conduction was derived in the radial direction only and the one dimensional conduction equation was solved analytically. Most recently, an elastic-plastic dynamic finite element model was presented by Tu et al. [25] to simulate temperature rise during bone drilling. They used the commercial finite element software ABAQUS® to estimate bone and drill-bit temperatures.

Thermo-mechanical effects in the process of *metal* drilling have been extensively studied and are well characterized in the literature [26–28]. Similar to those in bone drilling, the thermal effects in metal drilling are driven by heat generation due to material shearing through plastic deformations and various mechanisms of friction. The heat from the friction between the chip and rake face of the drill bit is significantly larger than the heat arising from both the friction between the drill-bit flank and the new cut surface of the workpiece (for a sharp tool) and that between the drill-bit periphery and the cylindrical surface of the drilled hole. Those friction mechanisms affect not only the instantaneous (local) heat generation, but also the tool wear and thermal changes in material properties. Depending on the scale of the analysis, one can define

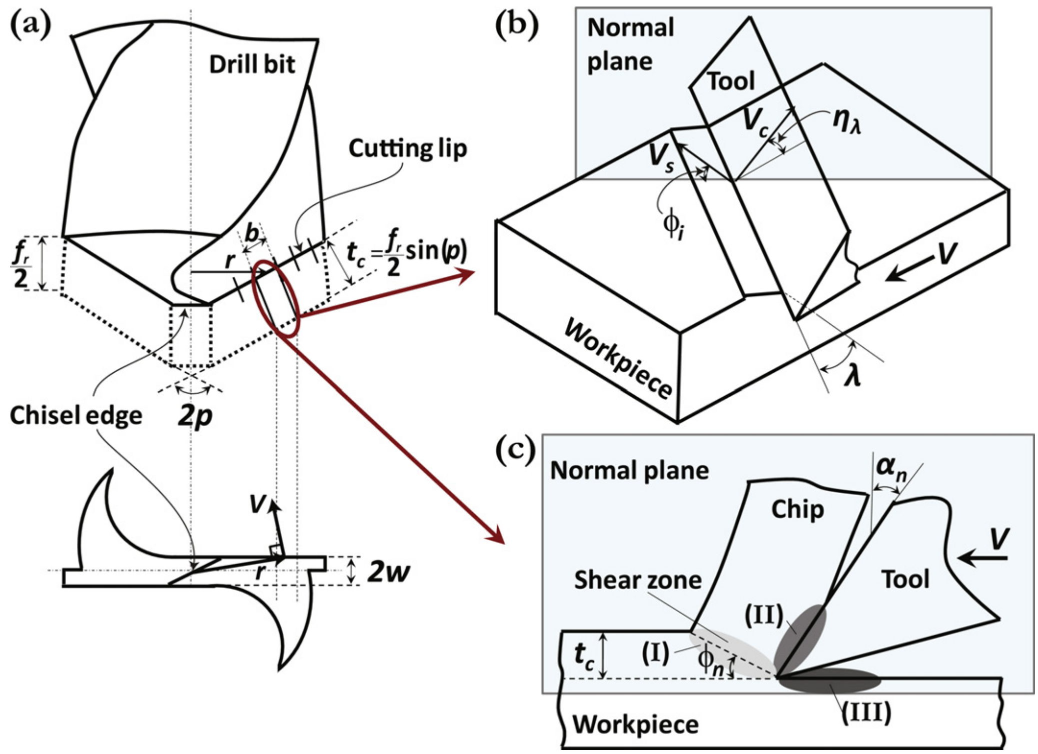

Fig. 2. Schematic illustration of cutting process in drilling: (a) a cutting element along the cutting lip, (b) the oblique cutting geometry that represent the cutting action at each cutting element, and (c) the normal plane (perpendicular to the cutting edge) that shows the cutting process with three main deformation zones, corresponding to major heat generation mechanisms: (I) shear (cutting) deformation within the shear zone, (II) friction between the rake face of the cutting tool and the chip, and (III) friction between the flank face of the cutting tool and the newly created surface of the workpiece.

more localized heat generation effects (such as by differentiating friction effects of the chip with the drill bit close to the cutting edge from further along the flute), but the overall effect of friction on the thermal behavior remains essentially the same.

While debate may exist in the literature about the relative significance of the various destructive effects associated with bone drilling, there appears to be a consensus that mathematical modeling of the coupled thermal-machining process is key to the decrease in tissue injury. Any approach to mathematical analysis of the associated thermo-mechanical effects of drilling must include at least three key elements: a constitutive law of heat transfer, characterization of the heat generation during drilling, and a numerical scheme to solve the mathematical representation of the physical process. The heat generation is the link between machining and the heat transfer process. In addition, the process of drilling makes the representation of heat transfer more complex, dealing with heat transfer in moving bodies. When reviewing the literature, one must appreciate the contribution of a specific study in context of advancing the state of knowledge in one or more of the above key elements. In this regard, the current study proposes a new constitutive model for heat transfer in the drill bit and the chip stream, assuming one dimensional axial temperature distribution of the combined thermal system. The current study uses established relationships of machining and heat generation from the literature. Finally, the current study proposes a new numerical scheme to solve heat transfer in the drill bit-chip stream system, but uses an available numerical scheme for conductive heat transfer in the bone. Hence, the main contribution of the current study is viewed as belonging to the modeling of thermal effects in bone drilling. This study is motivated by the need for a realistic and practical thermal model for the process of bone drilling, which will ultimately lead to improvement in drilling techniques and optimization of bone-drilling parameters. This paper presents the new model and provides a parametric study of selected drilling conditions on the thermal behavior during bone drilling. Although the model is applicable to bone drilling for both the cortical and the cancellous bones, the thermal and mechanical properties for the bovine cortical bone are used are used for the presented parametric study and sensitivity analysis.

2. Modeling

2.1. Heat generation

During the cutting process, a large portion of the cutting energy is converted into heat, which leads to elevation of temperature in the chips, the workpiece (bone), and the cutting tool (drill bit) [29]. With reference to the cutting operation illustrated in Fig. 2(c), heat generation during cutting mainly arises from three sources: (I) primary shear (cutting) deformation within the shear zone, (II) friction between the rake face of the cutting tool and the chip, and (III) friction between the flank face of the cutting tool and the newly created surface of the workpiece. With respect to heat generation in Zones I and II, the heat generated in Zone III is generally considered to be negligible for a sharp cutting tool [29].

Without loss of generality, it is assumed in this work that heat generation at the tip of the drill bit arises from the heat $\dot{Q}_{sh}$ due to shear deformation in the material within Zone I and from the heat $\dot{Q}_f$ due to the friction between the rake face of the tool and the chip within Zone II. Therefore, the total heat generated at the tip of the drill bit is obtained as $\dot{Q}_T = \dot{Q}_{sh} + \dot{Q}_f$. It is noted that the thermal model presented here is applicable regardless of the particular heat generation model used. Furthermore, the contribution to total heat from the small chisel edge is significantly smaller than that from the cutting lips, and will be neglected.[1]

As illustrated in Fig. 2, the cutting action experienced along the cutting lips is that of the oblique cutting process, where obliquity indicates that the cutting edge is inclined (with the angle λ) with respect to the normal to the cutting velocity V. The web thickness (chisel edge, see Fig. 1(b)) causes the cutting geometry (e.g., rake angle) to vary along the cutting lips. Furthermore, the magnitude of the cutting velocity and its orientation with respect to the cutting edge varies with the radius along the cutting lips. Therefore, in modeling the drilling process, the oblique cutting model is used along the cutting edge, where all the process parameters are functions of the cutting radius. In this work, we will consider the cutting lips to be divided into a finite number of cutting elements, each of which experiences the oblique cutting mechanics.

For a position along the cutting edge with the radius r, the heat generated within the primary shear zone (I) is considered to be proportional to the total shearing energy devoted to cutting. As such, the amount of heat arising from the cutting action at a cutting lip position with radius r can be expressed as

$$\dot{Q}_{sh}(r) = \zeta(r)\dot{Q}_s(r), \tag{1}$$

where $\dot{Q}_s(r)$ is the energy associated with the cutting process along the cutting lip location with radius r due to shearing of the material within the primary deformation zone, and $\zeta(r)$ is a constant indicating the portion of the shear energy that is converted into heat. The constant of proportionality is dependent upon the thermal properties of the tool, chip, and workpiece [30]. The constant of proportionality can be calculated as [29]

$$\zeta(r) = \begin{cases} 0.5 - 0.35\ \log(R_t(r)\tan\phi_n(r)) & \text{if}\quad 0.04 < R_t(r)\tan(\phi_n(r)) \le 10 \\ 0.3 - 0.15\ \log(R_t(r)\tan\phi_n(r)) & \text{if}\quad 10 < R_t(r)\tan(\phi_n(r)) \end{cases}, \tag{2}$$

where $\phi_n(r)$ is the normal shear angle which changes along the cutting lips. The thermal resistance $R_t(r)$ depends upon the cutting velocity, and is expressed as [29]

$$R_t(r) = \frac{1}{k}[\rho C_p t_c V(r)], \tag{3}$$

where k is the thermal conductivity of the workpiece, ρ is the density of the workpiece, and C_p is the specific heat of the workpiece, t_c is the uncut chip thickness, and $V(r)$ is the cutting (surface) speed at any point along the cutting lips. The cutting speed at radius r along the cutting edge can be calculated from the spindle speed n_s (in rpm) as $V(r) = 2\pi r n_s/60$.

Based on the oblique cutting theory, the shearing energy $\dot{Q}_s(r)$ arising from the shear deformation in the primary deformation zone is given as [23]

$$\dot{Q}_s(r) = F_s(r)V_s(r) = \tau_s(r)A_s(r)V_s(r), \tag{4}$$

where $F_s(r)$ is the shear force arising from the cutting lip at radius r, $A_s(r)$ is the shear area, $V_s(r)$ is the shear velocity, and $\tau_s(r)$ is the shear yield stress. Following [23], the shear yield stress during bone drilling is assumed to be

$$\tau_s(r) = 80\dot{\gamma}(r)^{0.06}, \tag{5}$$

where the shear (strain) rate $\dot{\gamma}(r)$ is given as [31]

$$\dot{\gamma}(r) = \frac{CV(r)}{t_c[\tan(\alpha_n(r)) + \cot(\phi_n(r))]}. \tag{6}$$

Here, α_n is the normal rake angle, and C is the material constant, value of which is taken to be equal to 6 [23,31]. Similarly to the cutting velocity, the normal rake angle $\alpha_n(r)$ and the shear angle $\phi_n(r)$ varies along the cutting lip as a function of the radius r.

Based on the minimum energy principle with the assumption that the primary shear zone is infinitesimally thin (i.e., to be a plane), Ernst and Merchant [32] calculated the shear angle as

$$\phi_n(r) = \frac{\pi}{4} + \frac{\alpha_n(r) - \beta_n}{2}. \tag{7}$$

where β_n is the friction angle for coefficient of friction μ on the rake face between the chip and the tool ($\mu = \tan\beta_n$). Note that $\mu = 0.751$ is used for bone drilling in the current study [23], and the friction angle β_n is assumed to be constant along the cutting lips. It is noted that the irrigation conditions could significantly affect the coefficient of friction on the rake face.

We will now consider a small element j along the cutting edge at radius r with a width (along the cutting edge) of b. For this element, the cutting-geometry parameters of uncut chip thickness, shear plane area, and width of cut can now be related to cutting conditions as

$$t_c = \frac{f_r/2}{n_s/60}\sin p, \quad A_s = \frac{bt_c}{\sin(\phi_n(r))\cos(\lambda(r))}, \tag{8}$$

and

$$b = \frac{(r_t - r_{ch})/N}{\sin\ p}, \tag{9}$$

respectively, where N is the total number of elements, f_r is the feed rate in mm/s, $2\,p$ is the point angle, r_t is the drill-bit radius, and r_{ch} is the chisel-edge radius. The inclination angle $\lambda(r)$ is obtained as

$$\lambda(r) = -\sin^{-1}\left(\left(\frac{w}{r}\right)\sin\ p\right), \tag{10}$$

where $2\ w$ is the web thickness of the drill bit. Furthermore, from the kinematics of the oblique cutting process, the shear velocity V_s along the cutting lip can be written as

$$V_s(r) = V(r)\frac{\cos(\alpha_n(r))\cos(\lambda(r))}{\cos(\phi_i(r))\cos(\phi_n(r) - \alpha_n(r))}, \tag{11}$$

where ϕ_i is the shear flow angle indicating the direction of shear within the shear plane. The shear flow angle can be obtained as,

$$\phi_i(r) = \tan^{-1}\left(\frac{\tan(\lambda(r))\cos(\phi_n(r) - \alpha_n(r)) - \tan(\eta_\lambda(r))\sin(\phi_n(r))}{\cos(\alpha_n(r))}\right). \tag{12}$$

In this equation, η_λ is the chip flow angle which varies along the cutting lip, and following Stabler's rule [19] the chip flow angle η_λ is assumed to be equal to the inclination angle λ.

Replacing r with $r_j = r_{ch} + j\Delta r$, where $\Delta r = (r_t - r_{ch})/N$, and combining Eqs. (4)–(11), the heat arising from the cutting element j due to the shearing in Zone I can be given as

$$\dot{Q}_{shj} = \zeta(r_j)F_s(r_j)V_s(r_j) = \frac{\zeta(r_j)\tau_s(r_j)t_c bV(r_j)\cos(\alpha_n(r_j))}{\sin(\phi_n(r_j))\cos(\phi_i(r_j))\cos(\phi_n(r_j) - \alpha_n(r_j))}. \tag{13}$$

Therefore, the heat generated due to the primary shearing (cutting) on each of the cutting lips can be written as

$$\dot{Q}_{sh} = \sum_{j=1}^{N}\dot{Q}_{shj}. \tag{14}$$

The heat generation arising from the friction between the chip and the tool (Zone II) will be calculated in a similar fashion. Unlike that of the shear deformation, where a portion of the energy is spent for shearing the material, in calculating the heat from the friction, the entire energy is converted into heat. Accordingly, the

[1] This is due to the small size of the chisel edge with respect to the cutting lips, very low cutting velocities experienced in the chisel edge, and thinned or split chisel edges observed in surgical drill bits.

heat generation due to friction in Zone II at a position along the cutting edge with radius r can be given as,

$$\dot{Q}_f(r) = F_f(r)V_c(r) = R(r)\sin(\beta_n)V_c(r), \tag{15}$$

where $F_f(r)$ is the friction force and $R(r)$ is the resultant (machining) force, which can be expressed as [18],

$$R(r) = \frac{F_s(r)}{\cos(\theta_n(r)+\phi_n(r))\cos(\theta_i(r))\cos(\phi_i(r))+\sin(\theta_i(r))\sin(\phi_i(r))}, \tag{16}$$

where $\theta_n(r) = \tan^{-1}(\tan(\beta_n)\cos(\eta_\lambda(r))) - \alpha_n(r)$ and $\theta_i(r) = \sin^{-1}(\sin(\beta_n)\sin(\eta_\lambda(r)))$.

The velocity of chip flow V_c can be related to cutting velocity as

$$V_c(r) = V(r)\frac{\sin(\phi_n(r))\cos(\lambda(r))}{\cos(\eta_\lambda(r))\cos(\phi_n(r)-\alpha_n(r))}. \tag{17}$$

Replacing r with $r_j = r_{ch} + j\Delta r$, and combining Eqs. (13)–(17), the heat arising from the friction energy at each element along the cutting lips can be expressed as

$$\dot{Q}_{fj} = F_f(r_j)V_c(r_j), \tag{18}$$

$$\dot{Q}_{fj} = \frac{V\tau_s t_c b\,\sin\beta_n\,\sin\phi_n\,\cos\lambda}{[\sin\phi_n\,\cos\lambda\,\cos(\theta_n+\phi_n)\cos\theta_i\,\cos\phi_i + \sin\theta_i\,\sin\phi_i]\cos\eta_\lambda\,\cos(\phi_n-\alpha_n)}. \tag{19}$$

The total friction heat generated due to the primary shearing (cutting) on each of the cutting lips can now be written as

$$\dot{Q}_f = \sum_{j=1}^{N}\dot{Q}_{fj}. \tag{20}$$

Finally, the amount of heat $\dot{Q}_T$ arising from each cutting lip can be expressed as

$$\dot{Q}_T = \dot{Q}_{sh} + \dot{Q}_f. \tag{21}$$

3. Mathematical model of heat transfer

The major difficulty in modeling heat transfer during drilling originates from the complex geometry of the drill bit, the relative motion of the drill bit and the workpiece, and the flow of a stream of chips along the drill-bit flutes. Since capturing thermal effects associated with the complex drilling process is quite challenging, and since some of those complexities are associated with different time and length scales, one can envision a simplified thermal model of a reduced complexity. For this purpose, the thermal model proposed here can be conveniently subdivided into two key systems: the drill bit-chip stream system, and the surrounding bone. The mathematical model for each system is presented separately – yet in a unified fashion – and the coupling of the two systems is described below.

3.1. Heat transfer in the drill bit-chip stream system

The underlying assumptions in formulating the drill bit-chip stream system are that: (1) the thermal conductivity of the drill bit is about two orders of magnitude higher than that of the bone (16.2 W/(m °C) for steel versus 0.54 W/(m °C) for bone [33], (2) the circumferential velocity of the drill bit is four to six orders of magnitude higher than its axial velocity, (3) the drill-bit diameter is much smaller than its length, and (4) the chip stream is well mixed. In the absence of more detailed information and without affecting the generality of the model, it is assumed that the chip packing ratio equals one, whereas the released fluid from the drilled bone perfectly fills the gaps between the solid bone chips. A variation in the packing ratio would affect the volumetric flow rate in the flute, which can be easily modified when experimental data become available. Under these assumptions, one may further assume negligible temperature variation in the circumferential direction, and negligible temperature gradients in the drill in the radial direction in comparison with temperature gradients in the bone in the same direction, whereas no general conclusion can be drawn with regard to the temperature gradients in the drill in the axial direction. It follows that the drill can be modeled as a thermal lumped capacity system in the radial direction and a distributed system in the axial direction-this combination is a unique contribution of the proposed modeling. Given this approach, the governing equation of the system is formulated with a typical control volume displayed in Fig. 3.

With reference to Fig. 3, the energy balance on a representative unit volume in the drill bit-chip stream system can be written as:

$$\dot{E}_{st} = \dot{Q}_{in,cond} + \dot{Q}_{in,conv} - \dot{Q}_{out,cond} - \dot{Q}_{out,conv} - \dot{Q}_{wall} - \dot{Q}_{cool} + \dot{Q}_{fric}, \tag{22}$$

where $\dot{E}_{st}$ is the rate of change of stored energy in the unit volume, $\dot{Q}_{cond}$ is the rate of heat transfer by conduction in the axial direction, $\dot{Q}_{conv}$ is the rate of convective heat transfer by the chip stream (positive value represents the direction of chip flow), $\dot{Q}_{fric}$ is the rate of heat generation due to friction between the drill-bit circumference and the wall of the hole, and this term is neglected in this study since $\dot{Q}_{fric}$ is assumed to be less dominant than heat generated at the drill-bit tip. $\dot{Q}_{wall}$ is the rate of heat transfer by conduction in the radial direction through the wall of the drilled hole, and $\dot{Q}_{cool}$ is the rate of drill bit cooling by convection, external to the drilled hole. In fact, $\dot{Q}_{cool}$ equals zero in the portion of the drill bit already in drilled hole (Fig. 3A), whereas $\dot{Q}_{fric}$, $\dot{Q}_{wall}$, and $\dot{Q}_{conv}$ equal zero in the portion of the drill bit outside of the drilled hole (Fig. 3B). The rate of change of stored energy in the unit volume is given by

$$\dot{E}_{st} = (\Omega\rho_c A_c \Delta z C_{p,c} + \rho_d A_d \Delta z C_{p,d})\frac{\partial T}{\partial t}, \tag{23}$$

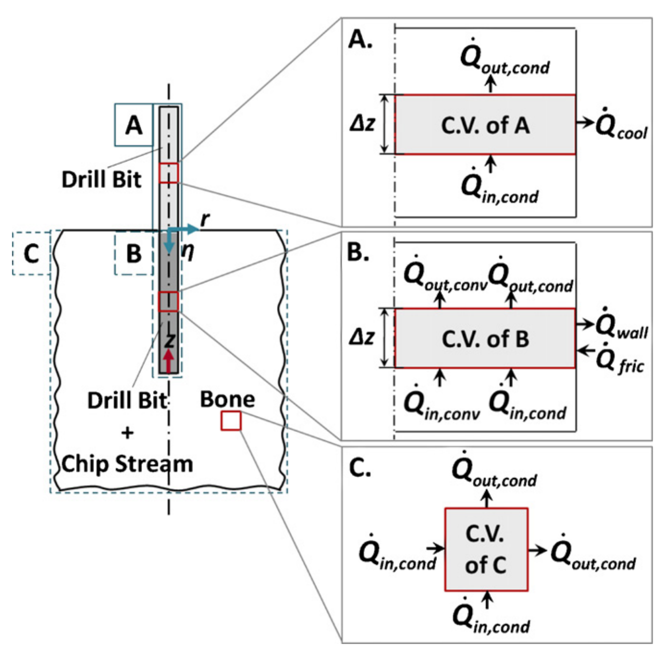

Fig. 3. Illustration of the typical control volumes used for mathematical formulation (A: the drill bit outside the bone, B: the drill bit inside the bone, and C: the bone).

where T is the temperature, t is the time, ρ is the density, z is the axial direction (its origin at the dead center of the drill bit and it is pointing toward the drill chuck), z is the height of the unit volume, A is the cross-sectional area (on the r–θ plane), C_p is the specific heat, the indices c and d represent the chip and the drill bit, respectively, and Ω indicates if the particular unit volume of the system is in contact with the bone (Fig. 3A; $\Omega = 0$) or not (Fig. 3B; $\Omega = 1$). Selecting $\Omega = 0$ for the external portion of the drill bit follows an assumption that chips are continually removed from the hole opening during the process of drilling. Note that the cross-section ratio of A_c to A_d is typically in the range of 3–7.

The net rate of conductive heat transfer along the axis of the system is given by

$$\dot{Q}_{in,cond} - \dot{Q}_{out,cond} = \frac{\partial}{\partial z}\left[(\Omega k_c A_c + k_d A_d)\frac{\partial T}{\partial z}\right]\Delta z, \tag{24}$$

where k is the thermal conductivity. The net rate of convective heat transfer by the stream of chips is given by

$$\dot{Q}_{in,conv} - \dot{Q}_{out,conv} = -\Omega \rho_c V_{ch} A_c C_{p,c}\frac{\partial T}{\partial z}\Delta z, \tag{25}$$

where V_{ch} is the axial velocity of the chip stream in the drill-bit flute. The rate of radial heat transfer by conduction through the wall of the hole is given by

$$\dot{Q}_{wall} = \Omega\left[-k_b 2\pi R \Delta z \left.\frac{\partial T}{\partial r}\right|_{r=R^+}\right], \tag{26}$$

where R is the radius of the drill bit, and the "+" sign indicates that the temperature gradient is evaluated at the wall from the bone side (e.g., the adjacent system), which, in fact, represents the coupling of the drill bit-chip stream system with the bone system (described separately in the next subsection); the bone system is notated with the index b. Note that the radial temperature gradient within the drill bit cannot be evaluated since the temperature is lumped in this direction. Further note that, since the energy balance for the system is the basis for formulation, the lumped temperature is representative of the average temperature, regardless of the inability to trace the actual radial temperature variation.

Outside of the drilled hole, the drill bit is cooled by the surroundings

$$\dot{Q}_{cool} = (1 - \Omega) h 2\pi R (T - T_\infty)\Delta z, \tag{27}$$

where h is the coefficient of heat transfer to the surroundings and T_∞ is the surroundings temperature. The heat balance equation, Eq. (22), can now be rewritten in terms of all the specific quantities presented in Eqs. (23)–(27) as follows

$$(\Omega \rho_c A_c C_{p,c} + \rho_d A_d C_{p,d})\frac{\partial T}{\partial t} = (\Omega k_c A_c + k_d A_d)\frac{\partial^2 T}{\partial^2 z} - \Omega \rho_c A_c C_{p,c}\frac{\partial T}{\partial z}$$
$$+ 2\Omega k_b \pi R \left.\frac{\partial T}{\partial r}\right|_{r=R^+} + 2(\Omega - 1) h \pi R (T - T_\infty) + \dot{Q}'_{fric}, \tag{28}$$

after dividing the entire equation by the small but finite quantity Δz, where $\dot{Q}'_{fric}$ is the rate of heat generation by friction per unit length of the drill bit. Eq. (28) represents an implicit model assumption of uniform and constant physical properties in the respective materials.

Two boundary conditions are assumed in the axial direction of the drill bit-chip stream system: a known temperature at the drill chuck, and a known heat flux at the cutting edge of the drill bit, as discussed in more detail in the next subsection. The initial temperature of the drill bit is assumed uniform, having the same value as the drill chuck through the process of drilling.

3.2. Heat transfer in the bone

With reference to Fig. 3, heat transfer in the bone can be represented as a simple heat diffusion equation:

$$\frac{1}{r}\frac{\partial}{\partial r}\left(r\frac{\partial T}{\partial r}\right) + \frac{\partial^2 T}{\partial \eta^2} = \frac{1}{\alpha_b}\frac{\partial T}{\partial t}, \tag{29}$$

where η is the axial coordinate of the cylindrical system and α is the thermal diffusivity. The relative motion of the drill bit-chip stream system to the bone is given by:

$$\eta = L - V_d t, \tag{30}$$

where L is the thickness of the specimen and V_d is the velocity of drill-bit penetration. The boundary condition at the drill-bit tip ($z = 0$) is given by:

$$\dot{Q}_T = -(k_d A_d + k_c A_c)\left.\frac{\partial T}{\partial z}\right|_{z=0} + k_b (A_d + A_c)\left.\frac{\partial T}{\partial \eta}\right|_{\eta=\eta_d}, \tag{31}$$

where η_d is the instantaneous location of the drill-bit tip in the bone coordinate system. Due to the sparse vascular network and the relatively low blood perfusion in the bone, the potential cooling effect of blood perfusion is assumed negligible in the current study. Nevertheless, if one assumes a significant cooling effect due to blood perfusion, Eq. (29) could be replaced with the classical bioheat equation – also known as Pennes' equation – without affecting the generality of the model proposed in the current study.

In the thermal sense, the bone system is assumed semi-infinite in the radial direction, representing a much larger thermal system than the drill diameter. In this context, a one-dimensional physical domain may be assumed semi infinite in the thermal sense as long as the thermal information due to thermal events on one of its boundaries has not propagated through the domain to the further boundary. In practice, a system diameter larger than ten times the drill diameter approaches that definition of semi infinity but, nonetheless, it is problem dependent. In the axial direction, the system may be assumed semi-infinite or finite with convective boundary condition on its distant boundary, based on the particular problem setup. Note that the length L in Eq. (30) refers to the thickness of the physical system and not to the penetration depth on the thermal information. Quantification of those semi-infinite assumptions is presented in the discussion section. Heat transfer by convection is assumed between the bone surface and the surroundings. The initial condition at the bone is assumed to be uniform temperature.

4. Numerical solution

Governing Eqs. (28) and (29), subject to the internal boundary condition presented by Eq. (31), were simultaneously solved using an explicit finite-difference method [34]. This numerical scheme is first order in time, second order in space, and conditionally stable. At any given time level, the temperature distribution in the drill bit-chip stream system was solved first, Eq. (28), subject to its boundary conditions from the previous time-level calculations. Next, the temperature at the drill-bit tip was updated, and the temperature distribution in the bone domain was calculated, Eq. (29). This process was repeated at each time level as the transient process progresses.

While the coupling boundary condition presented in Eq. (31) has been maintained at each time level, the actual location where it is calculated has been continuously updated. While this boundary condition is always implemented at $z = 0$, segments of grid points are continually removed from the bone domain within radius R under the drill bit, to represent material removal. The current location of the drill-bit tip in the bone is given by Eq. (30), which was

Table 1
Thermal properties of (cortical) bone of bovine femur and drill bit used in this work.

	Bone [33]	Drill bit (316L stainless steel)
Thermal conductivity (W/mK)	0.54	16.2
Specific heat (J/(kg K))	1260	502.4
Density (kg/m^3)	1800	8030

used to eliminate grid points from the mesh and update the formulation of the boundary condition in Eq. (31).

For the specific calculations presented in this report, the drill bit has been subdivided into 1000 grid points, and the surrounding bone to a 300 × 400 array of grid points.

Numerical examples displayed in this report were all generated for a bone domain diameter of 30 mm and height of 15 mm. A drill bit diameter of 3.5 mm and 50 mm length were further selected (typical to orthopaedic surgery). Given stability requirements [34] and material properties (see Table 1), a typical time step of 10^{-6} s was selected.

5. Sensitivity analysis

A sensitivity analysis was performed to investigate the contribution of the unique features of the new thermal model given in Eq. (28) on the rate of heat transfer and the resulting temperature field.

The sensitivity analysis was focused on three key features: the effect of heat transfer along the drill-bit flutes by the chip stream, the effect of cooling the drill bit by external means, and the effect of initial conditions on the resulting temperature field.

The sensitivity analysis cases were performed in initial conditions of 20 °C in the drill bit and 37 °C in the bone with a standard drill bit, having the following parameters: diameter of 3.5 mm, length of 50 mm, point angle of 90°, helix angle of 23°, and a feed rate of 2 mm/s. The domain of the bone specimen was 15 mm by 15 mm. The thermal properties used for the sensitivity analysis are listed in Table 1.

5.1. Heat transfer along the drill-bit flute

Fig. 4(a) displays the variation of the maximum temperature at the drill-bit tip with the progression of drilling at a spindle speed of 2400 rpm in two representative cases: when the heat transfer by convection is neglected (V_{ch} in Eq. (25) is set to zero), and when the convective heat transfer is fully taken into account. Fig. 4(a) also displays the rate of heat transfer generated by the stream of chips (right vertical axis), as calculated from Eq. (25). It can be seen from Fig. 4(a) that the maximum tip temperature increases with the increasing drilling depth, regardless of whether the convective term is accounted for or not. At 9 mm depth, which is the maximum drilling depth investigated here, the convective term reduces the tip temperature by 5.9 °C (the tip temperature is 66.2 °C and 60.3 °C for the cases of no convection and convection, respectively).

5.2. Cooling the drill bit by external means

Fig. 4(b) displays the variation of the maximum temperature as a function of the spindle speed for three typical cases of drilling: (1) the external portion of the drill bit is cooled by convection to the surrounding air, (2) the external portion of the drill bit is cooled by saline, and (3) an infinite heat transfer rate exists between the external portion of the drill bit and the surroundings.

Case (3) represents an upper limit to cooling at the external portion of the drill bit. The heat transfer coefficient by convection has been calculated using the experimental correlation [35],

$$\overline{\mathrm{Nu}} = 0.1\,\mathrm{Re}_r^{2/3} \quad \text{and} \quad \mathrm{Re}_r = \frac{(N/60)(D_d)^2\rho_{air}}{2\mu_{air}}, \tag{32}$$

where $\overline{\mathrm{Nu}}$ is the average Nusselt number, Re_r is the rotating Reynolds number, μ is the dynamic viscosity and the index *air* represent the air. This correlation yields heat transfer coefficient values in the range of 18.8 at 3000 rpm to 55.0 at 15,000 rpm for air, 2639.3 at 3000 rpm to 7717.4 at 15,000 rpm for saline (thermal properties similar to water), and infinite value for Case (3). It can be seen from Fig. 4(b) that the maximum tip temperature decreases with the increasing value of the heat transfer coefficient by convection at any depth of drilling. Note that the heat transfer coefficient by convection is of the order of 10^1 W/(m^2 °C) and 10^3 W/(m^2 °C) for air and saline, respectively. For all cases, the maximum tip temperature increases with the increasing spindle speed and, independently, with the depth of drilling. Both effects could be expected since the heat generation increases with the cutting speed, and the cooling effect diminishes as the location of heat generated becomes more distant to the cooled portion of the drill bit. At 15,000 rpm and 9 mm depth, for example, the maximum temperatures are 64.7 °C, 67.4 °C, and 68.1 °C, for the cases of an infinite heat transfer coefficient by convection, saline cooling, and air-cooling,

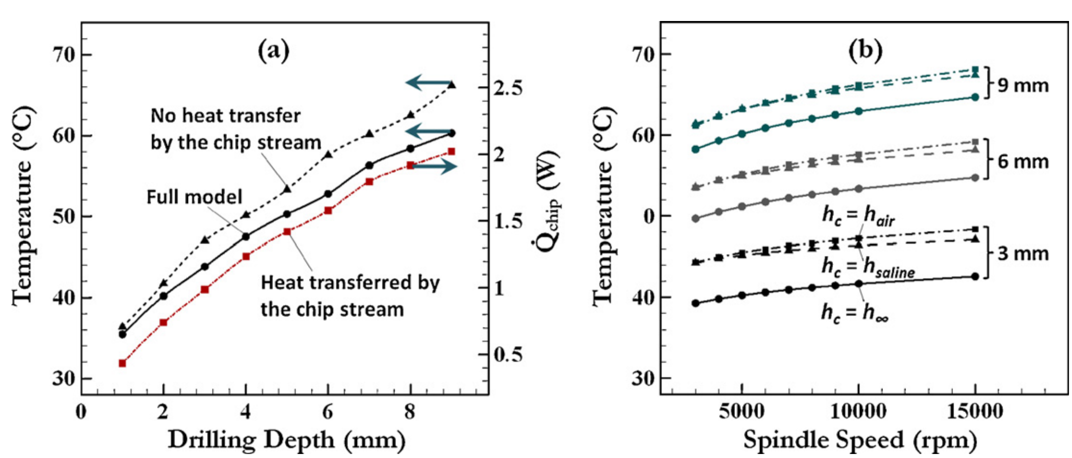

Fig. 4. Variation of the maximum temperature due to chip removal and drill-bit cooling effects: (a) maximum temperature as a function of drilling depth with and without the cooling effect of the chip stream for three drilling depths. The horizontal arrows indicate the applicable axis for each curve, and (b) maximum temperature as a function of spindle speed for three cases of drill-bit cooling and three drilling depths: (1) to the surrounding air, (2) to a surrounding saline, and (3) to an extremely high flow rate of the coolant. All values are calculated for initial temperatures of 20 °C and 37 °C for the drill bit and bone, respectively, when using a 3.5 mm diameter drill bit having a point angle of 90° and helix angle of 23°.

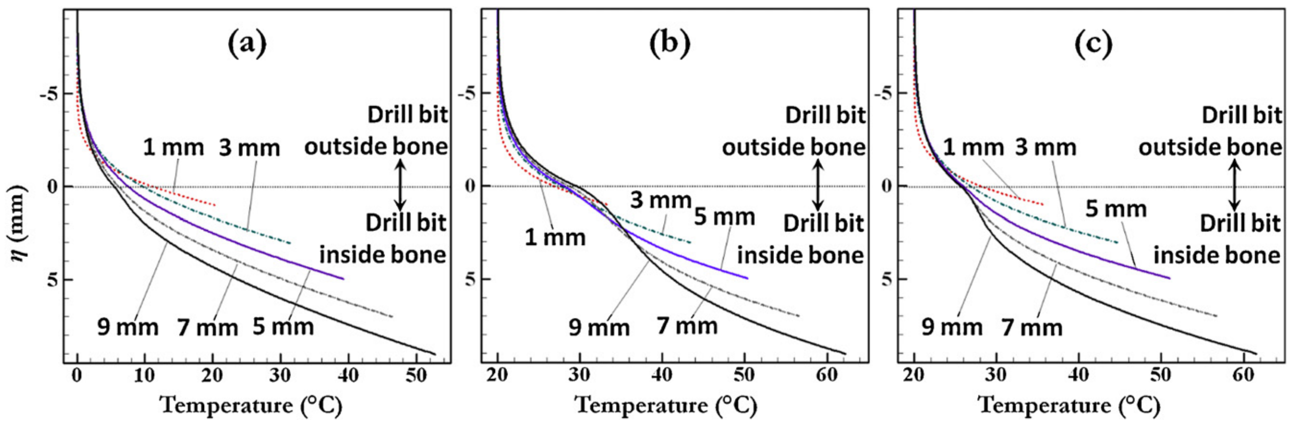

Fig. 5. Temperature distribution along the drill bit in three initial-condition cases: (a) 0 °C at the drill bit and 37 °C in bone, (b) 20 °C in the drill bit and 20 °C in the bone, and (c) 20 °C in the drill bit and 37 °C in the bone; calculated for a 3.5 mm diameter drill bit having a point angle of 90° and helix angle of 23°. Note that the direction of η was selected to be consistent with all other illustrations.

respectively. At 3000 rpm and 9 mm depth as another example, the maximum temperatures are 58.2 °C, 61.4 °C, and 63.2 °C, for the cases of an infinite heat transfer coefficient by convection, saline cooling, and air-cooling, respectively. While the specific biological response to thermal exposure is beyond the scope of the current study, in terms of an overall effect, the difference between 58.2 °C and 68.1 °C may be the difference between mild hyperthermic conditions and thermal ablation, depending on the exposure time to elevated temperatures. This range of temperatures signifies the need for a more precise modeling of bioheat transfer during bone drilling.

5.3. The effect of initial condition

Fig. 5 displays the axial temperature distributions in the drill bit and bone for three representative cases: (a) initial temperatures of 0 °C and 37 °C for the drill bit and the bone, respectively; (b) initial temperatures of 20 °C and 20 °C for the drill bit and the bone, respectively; and, (c) initial temperatures of 20 °C and 37 °C for the drill bit and the bone, respectively. Note that the chuck temperature is always assumed to remain at initial temperature of the drill bit.

Note that Case (b) is simulative of bench-top experiments, and is included here for comparison purposes. Further note that this is the only case where the initial condition of both the drill and the bone are identical, where temperature elevation here is solely due to heat generation during drilling.

The spindle speed and feed rate were maintained constant in all cases at values of 2400 rpm and 2 mm/s, respectively. Fig. 6 displays the resulting temperature fields for the above cases when the drill bit reaches a depth of 9 mm. The dramatic effect of drill bit cooling can be observed in Figs. 5 and 6. The maximum drill-bit temperature is 51.6 °C in Case (a), and it reaches 60.3 °C in Case (c).

Fig. 7 displays the axial temperature distribution in the drill bit and the bone. There are two major differences between Figs. 5 and 7: the temperature distribution in Fig. 5 includes the drill bit only, whereas the temperature distribution in Fig. 7 also includes the bone. With reference to Cases (a) and (c) in Fig. 7, it can be seen that early on in the drilling process (at a depth of 1 mm for example), despite the generated heat at the drill-bit tip, the drill bit may have an overall cooling effect – lowering the temperature in the bone below its initial value. Only at a more advanced stage (7 mm for Case (a) and 3 mm for Case (c)), the maximum temperature becomes the temperature at the tip.

It can also be seen that at an intermediate stage, the tip temperature may exceed the initial temperature of the bone, but the bone in close proximity to the temperature of the drill-bit tip may be lower than the bone's initial temperature, reminiscence of the initial cooling effect of the drill bit. This effect may explain the lower temperature area ahead of the drill bit in Case (a) of Fig. 6. This analysis further signifies the need for a detailed thermal analysis of bone drilling for identification of the thermal history in the bone.

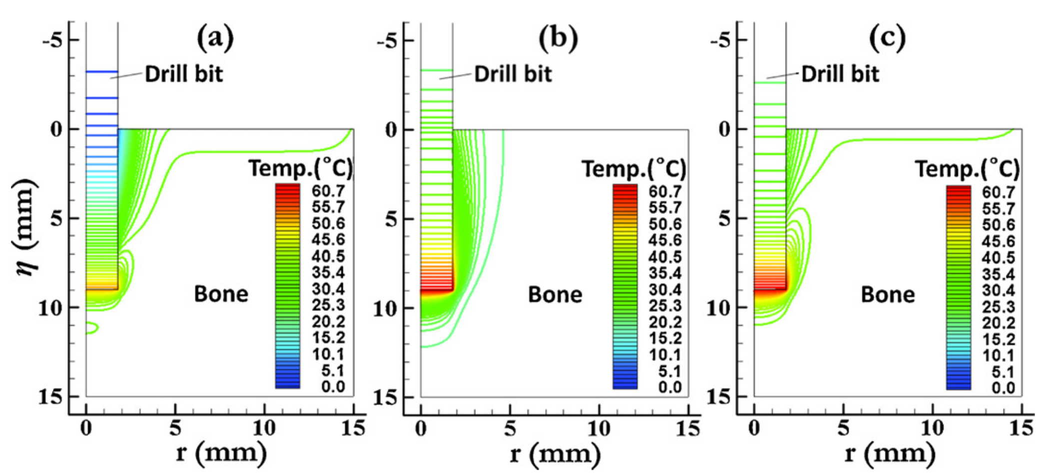

Fig. 6. Temperature field in the bone when the drill bit reaches a depth of 9 mm, following three initial-condition combinations: (a) 0 °C at the drill bit and 37 °C in bone, (b) 20 °C in the drill bit and 20 °C in the bone, and (c) 20 °C in the drill bit and 37 °C in the bone; calculated for a 3.5 mm in diameter drill bit having a point angle of 90° and helix angle of 23°.

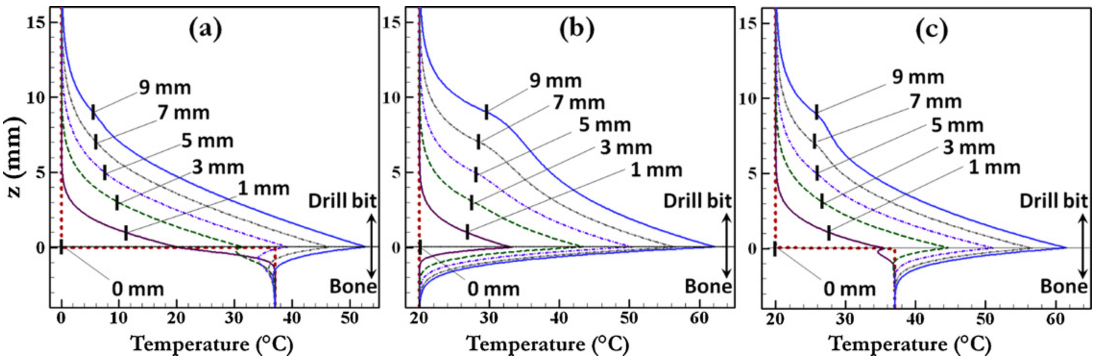

Fig. 7. Temperature distribution along the axis of the system (drill bit and bone) in three initial-condition cases: (a) 0 °C at the drill bit and 37 °C in bone, (b) 20 °C in the drill bit and 20 °C in the bone, and (c) 20 °C in the drill bit and 37 °C in the bone; calculated for a 3.5 mm diameter drill bit having a point angle of 90° and helix angle of 23°. Note that the vertical solid bars indicate the temperature when the drill bit reaches the point.

6. Parametric studies

Using the new model proposed in the current study, a parametric investigation was performed to identify how drilling conditions and drill-bit geometry affect the maximum temperature during bone drilling. This parametric investigation includes the spindle speed, feed rate, drill-bit diameter, point angle, and helix angle. The spindle speed and the feed rate were varied from 400 rpm to 3000 rpm and 0.42 mm/s to 3.3 mm/s, respectively, consistent with the literature [1,5,10]. The drill-bit diameter was varied in the range of 1.5 mm and 4.5 mm, consistent with orthopaedic-surgery practice. The point angle was examined in the range of 70–130°, consistent with the literature [10,11]; note that a point angle of 118° is frequently used in metal cutting. The helix angle was investigated in the range of 12–38°, also consistent with the literature [2,7]. The current investigation focuses on drilling to a maximum depth of 9 mm, which is typical thickness of the cortical portion of bone, especially for bovine femur or tibia.

Fig. 8 displays the resulting temperature field in at various depths, subject to a spindle speed of 2400 rpm and a feed rate of 2 mm/s, when using a 3.5 mm diameter stainless-steel drill-bit with a point angle of 90° and a helix angle of 23°. The initial temperature of the drill bit and the bone was 20 °C and 37 °C, respectively, and the temperature of the drill bit gradually increase up to 60.3 °C at 9 mm depth as the drilling progresses. This case study was selected as the reference for the following parametric study, with the results displayed in Fig. 9.

As shown in Fig. 9(a), the maximum temperature increases with the increasing spindle speed, when all the other parameters are held constant, subject to the initial temperatures of 20 °C and 37 °C for the drill bit and bone, respectively, a feed rate of 2 mm/s, when using a 3.5 mm diameter stainless-steel drill-bit with a point angle of 90° and a helix angle of 23°. This trend has been noted from several experimental studies [8,9,13]. The maximum simulated temperature at 9 mm ranges from 54.3 °C at 400 rpm to 61.1 °C at 3000 rpm, which is clearly within the hyperthermic temperature range. In fact, for all the studied cases, the tip temperature in regions deeper than 6 mm is already in the hyperthermic temperature region. Of course, the expected thermal injury is a combination of temperature and exposure time (in some literature referred to as "thermal dose"), which is beyond the scope of the current study. The current study, however, warrants a follow-on investigation on the effect of the thermal history on thermal damage during bone drilling. Hillery and Shuiab [11] mentioned that if the temperature rises above 55 °C for a period of longer than half a minute, bone endures serious damage. At a temperature of 45 °C serious damage only occurs after 5 h of exposure. Based on this criterion, the spindle speeds of 400 rpm at the feed rate 2 mm/s used in the simulations is likely to be accepted for bone drilling operation.

It can be seen from Fig. 9(b) that the maximum temperature increases rapidly with increasing feed rate, when all other parameters are held constant, subject to the initial temperatures of 20 °C and 37 °C for the drill bit and bone, respectively, a spindle speed of 2400 rpm, when using a 3.5 mm diameter stainless-steel drill-bit

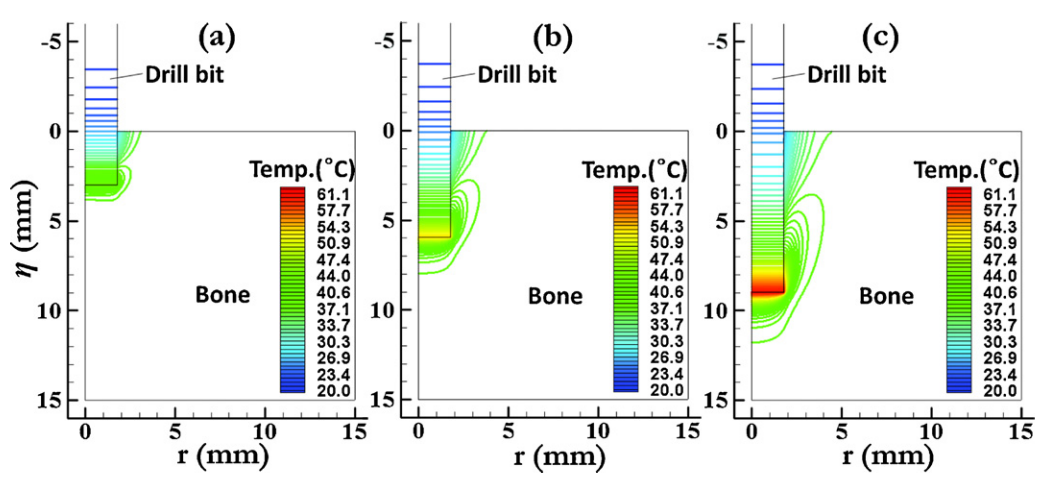

Fig. 8. Temperature field in the bone when the drill bit reaches a depth of (a) 3 mm, (b) 6 mm, and (c) 9 mm. The values are calculated for the initial temperatures of 20 °C and 37 °C for the drill bit and bone, respectively, for a 3.5 mm diameter drill bit having a point angle of 90° and helix angle of 23°.

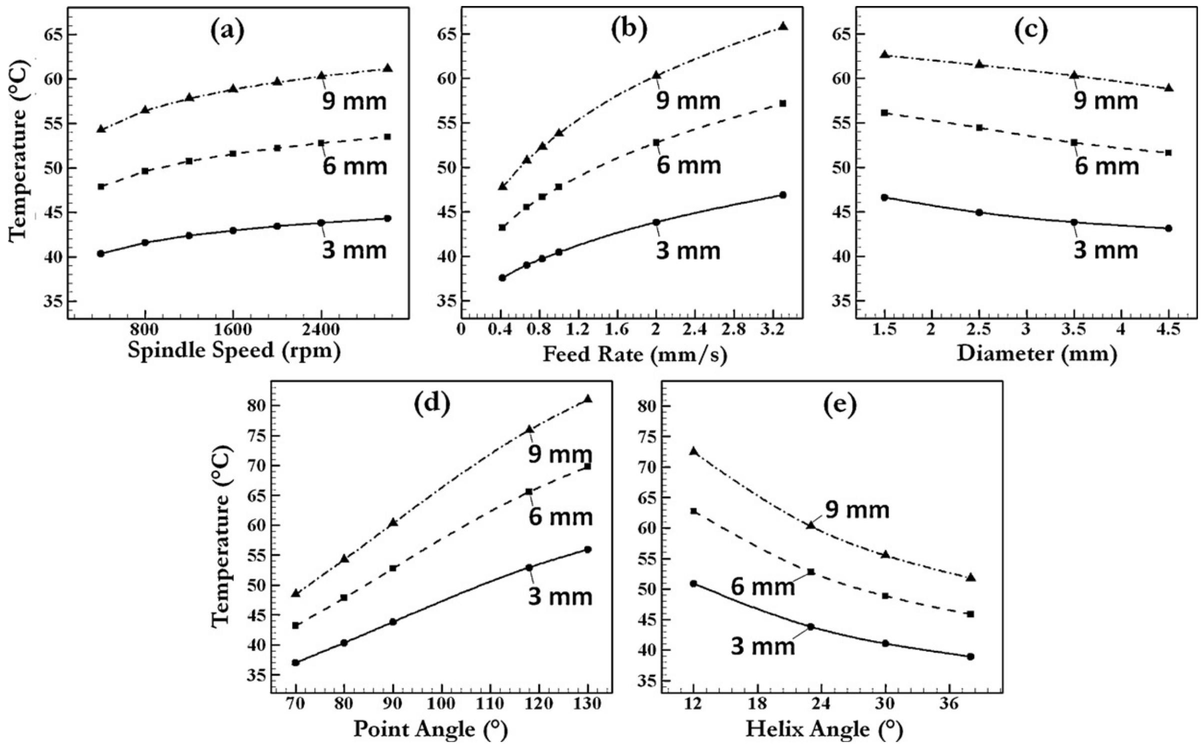

Fig. 9. The variation of maximum temperature with (a) spindle speed, (b) feed rate, (c) drill-bit diameter, (d) point angle of the drill bit, and (e) helix angle of the drill bit. All values are calculated for the initial temperatures of 20 °C and 37 °C for the drill bit and bone, respectively. For all parameters other than the studied parameter, the following nominal values are used: 2400 rpm spindle speed, 2 mm/s feed rate, 3.5 mm diameter, 90° point angle, 23° helix angle. Calculations are completed for a stainless steel drill bit.

with a point angle of 90° and a helix angle of 23°. At higher depths, even relatively low feed rates may cause the maximum temperature to exceed the thermal ablation threshold, commonly taken as 56 °C; at such high temperatures, the exposure time to thermal injury is measured in seconds. For example, the maximum temperature is simulated to be 47.7 °C at a feed rate of 0.42 mm/s and a depth of 9 mm. Increasing the feed rate to 3.3 mm/s increases the maximum temperature to 65.8 °C at the same depth of 9 mm. This strong dependence of the feed rate is a result of significant increase in generated heat due to increased feed. Although the process is completed in a much shorter time, thereby reducing the effect of heat on the bone, the increase in heat generation due to increased feed is considerably dominant.

The effect of drill-bit diameter on the maximum temperature for the initial temperatures of 20 °C and 37 °C for the drill bit and bone, respectively, for a stainless-steel drill-bit having a point angle of 90° and helix angle of 23° is shown in Fig. 9(c). It is seen that the maximum temperature decreases slightly with the increasing drill-bit diameter. For example, the maximum temperature ranges from 62.6 °C to 58.8 °C, at 9 mm depth, for a range of 1.5 mm to 4.5 mm of a drill-bit diameter. This effect can be explained by the higher heat conduction capability of larger drill bit, where the drill bit serves as a cooling element (see Fig. 6 and related discussion about the drill bit's cooling capability). It is also noted that a larger drill bit creates a larger chip-stream flow, which contributes to heat removal from the machined area (see Fig. 4(a) and related discussion about the cooling effect of the chip stream).

As seen in Fig. 9(d), the maximum temperature show a strong dependence upon the point angle, larger point angles producing significantly higher maximum temperatures. At the reference conditions (a spindle speed of 2400 rpm, a feed rate of 2 mm/s, and a stainless-steel drill-bit diameter of 3.5 mm having a helix angle of 23° for the initial temperatures of 20 °C and 37 °C for the drill bit and bone, respectively), the maximum temperature at a depth of 9 mm varied from 48.5 °C to 80.9 °C as the point angle was changed from 70° to 130°, respectively. This effect is expected since larger point angles induce higher shear deformations to the material, causing increased heat generation.

Four different helix angles were examined in the simulation, including 12°, 23°, 30°, and 38°. The reference conditions were a spindle speed of 2400 rpm, a feed rate of 2 mm/s, and a stainless-steel drill-bit diameter of 3.5 mm having a point angle of 90° for the initial temperatures of 20 °C and 37 °C for the drill bit and bone, respectively. As shown in Fig. 9(e), the maximum temperature decreased as the helix angle increased. At 9 mm depth, the maximum temperature ranges from 72.5 °C to 51.8 °C for the helix angle range of 12–38°. The simulation results show an agreement with the suggestion provided by Natali et al. [7], who suggested the use of a fast helix (high helix angle) for reducing thermal damage in bone drilling. In the simulations, the highest maximum temperature (72.5 °C) occurred at the helix angle of 12°, contrary to the recommendation by Fuchsberger [2], who suggested a helix angle from 12° to 14° for bone drilling.

Based on the results displayed in Fig. 9, it can be concluded that the maximum temperature in bone drilling can be reduced by selecting lower spindle speeds, lower feed rates, larger drill-bit diameters (if possible), smaller point angles, and higher helix angles. As expected, the deeper the drilled hole, the higher will be the maximum temperature.

7. Summary and conclusions

A new thermal model for bone drilling has been presented with applications to orthopaedic surgery. The new model combines a unique heat-balance equation in the drill bit-chip stream system, an ordinary heat diffusion equation in the bone, and heat generation at the drill-bit tip based on established machining theory. The new model is solved numerically, using a tailor-made finite-difference scheme for the drill bit-chip stream system, coupled with a classic finite difference method for the bone.

A sensitivity analysis of the new model by means of computer simulations indicated that heat transfer along the flutes must be taken into account. It contributes to cooling of the drill-bit tip, and hence, the bone in the vicinity of the drill-bit tip, and reduces the maximum temperature with potential implications on thermal injury. Heat transfer by the chip stream was integrated as a convective effect into the model. The sensitivity analysis further showed that drill bit cooling may have a significant effect on the maximum drill-bit temperature, even in an advanced stage of drilling, where the tip is distant to the cooled portion of the drill bit. Finally, the sensitivity analysis showed that the maximum temperature of the drill bit is influenced by its initial temperature.

A parametric study with the new model has been conducted to investigate the dependency of the maximum temperature upon the spindle speed, feed rate, drill-bit diameter, point angle, and helix angle. The results of the parametric study indicate that the maximum temperature depends strongly on the hole depth, feed rate, point angle, and helix angle. Higher maximum temperatures were observed at higher feed rates, higher point angles, and lower helix angles. The effect of spindle speed and drill diameter were seen to be weaker; higher spindle speeds and smaller drill diameters produced higher maximum temperatures. The proposed model can be used to investigate optimal machining conditions and drill-bit geometries, which reduce thermal damage in the bone drilling process.

Acknowledgements

This work was supported by Dowd-ICES fellowship in Carnegie Mellon University. The authors wish to thank Ph.D. student Nithyanand Kota for his assistance in deriving the heat-generation formulation.

Conflict of interest statement

The authors declare that no conflicts of interest associated with the presented work.

References

[1] Bachus KN, Rondina MT, Hutchinson DT. The effects of drilling force on cortical temperatures and their duration: an in vitro study. Medical Engineering and Physics 2000;22(10):685–91.
[2] Fuchsberger A. The damaging temperature at the machining of bone. Unfallchirurgie 1988;14(4):173–83.
[3] Augustin G, Davila S, Udiljak T, Vedrinal DS, Bagatin D. Determination of spatial distribution of increase in bone temperature during drilling by infrared thermography: preliminary report. Archives of Orthopaedic and Trauma Surgery 2009;129(5):703–9.
[4] Kreith K. The CRC handbook of thermal engineering. CRC Press; 2000. p. 4–152.
[5] Brisman DL. The effect of speed, pressure, and time on bone temperature during the drilling of implant sites. Internation Journal of Oral and Maxillofacial Implants 1996;11(1):35–7.
[6] Eriksson AR, Albrektsson T, Albrektsson B. Heat caused by drilling cortical bone: temperature measured in vivo in patients and animals. Acta Orthopaedica Scandinavica 1984;55(6):629–31.
[7] Natali CN, Ingle P, Dowell J. Orthopaedic bone drills—can they be improved?: temperature changes near the drilling face. Journal of Bone and Joint Surgery 1996;78-B(3):357–62.
[8] Matthews LS, Green CA, Goldstein SA. The thermal effects of skeletal fixation-pin insertion in bone. Journal of Bone and Joint Surgery 1984;66(7):1077–83.
[9] Saha S, Pal S, Albright J. Surgical drilling: design and performance of an improved drill. Transactions of ASME, Journal of Biomechanical Engineering 1982;104(3):245–52.
[10] Augustin G, Davila S, Mihoci K, Udiljak T, Vedrinal DS, Antabak A. Thermal osteonecrosis and bone drilling parameters revisited. Archives of Orthopaedic and Trauma Surgery 2008;128(1):71–7.
[11] Hillery MT, Shuaib I. Temperature effects in the drilling of human and bovine bone. Journal of Materials Processing Technology 1999;92–93:302–8.
[12] Mellinger JC, Ozdoganlar OB, Devor RE, Kapoor SG. Modeling chip-evacuation forces and prediction of chip-clogging in drilling. Transactions of ASME, Journal of Manufacturing Science and Engineering 2002;124(3):605–14.
[13] Toews AR, Bailey JV, Townsend HGG, Barber SM. Effect of feed rate and drill speed on temperatures in equine cortical bone. American Journal of Veterinary Research 1999;60(8):942–4.
[14] Ohashi H, Therin M, Meunier A, Christel P. The effect of drilling parameters on bone. Journal of Material Science: Materials in Medicine 1994;5(4):225–31.
[15] Nam O, Yu W, Choi MY, Kyung HM. Monitoring of bone temperature during osseous preparation for orthodontic micro-screw implants: effect of motor speed and pressure. Key Engineering Materials 2006;321–323:1044–7.
[16] Abouzgia MB, Symington JM. Effect of drill speed on bone temperature. International Journal of Oral and Maxillofacial Surgery 1996;25(5):394–9.
[17] Sharawy M, Misch CE, Weller N, Tehemar S. Heat generation during implant drilling: the significance of motor speed. Journal of Oral and Maxillofacial Surgery 2002;60(10):1160–9.
[18] Shamoto E, Altintas Y. Prediction of shear angle in oblique cutting with maximum shear stress and maximum energy principles. Journal of Manufacturing Science and Engineering 1999;121:399–407.
[19] Stabler GV. The fundamental geometry of cutting tools. Proceedings of the Institution of Mechanical Engineers 1951;165:14–26.
[20] Boyne PJ. Histologic response of bone to sectioning by high-speed rotary instruments. Journal of Dental Research 1966;45(2):270–6.
[21] Costich ER, Youngblood PJ, Walden JM. A study of the effects of high-speed rotary instruments on bone repair in dogs. Oral Surgery, Oral Medicine, and Oral Pathology 1964;17:563–71.
[22] Rafel SS. Temperature changes during high-speed drilling on bone. Journal of Oral Surgery, Anesthesia, and Hospital Dental Service 1962;20:475–7.
[23] Davidson SRH, James DF. Drilling in bone: modeling heat generation and temperature distribution. Transactions of ASME, Journal of Biomechanical Engineering 2003;125(3):305–14.
[24] Kalidindi V. Optimization of drill design and coolant system during dental implant surgery. MS thesis, University of Kentucky, Lexington, KY; 2004.
[25] Tu YK, Tsai HH, Chen LW, Huang CC, Chen YC, Lin LC. Finite element simulation of drill bit and bone thermal contact during drilling. In: Proceedings of the 2nd International Conference on Bioinformatics and Biomedical Engineering. 2008.
[26] DeVries MF, Saxena UK, Wu SM. Temperature distributions in drilling. Transactions of ASME, Journal of Engineering for Industry 1968;90:231–8.
[27] Saxena UK, DeVries MF, Wu SM. Drill temperature distributions by numerical solutions. Transactions of ASME, Journal of Engineering for Industry 1971;93(4):1057–66.
[28] Watanabe K, Yokoyama K, Ichimiya R. Thermal analyses of the drilling process. Bulletin of the Japan Society of Precision Engineering 1977;11(2):71–7.
[29] Boothroyd G. Temperatures in orthogonal metal cutting. Proceedings of the Institution of Mechanical Engineers 1963;177:789–810.
[30] Agapiou JS, DeVries MF. On the determination of thermal phenomena during drilling. Part I. analytical models of twist drill temperature distributions. International Journal of Machine Tools and Manufacture 1990;30(2):203–15.
[31] Tay AO, Stevenson MG, Davis GV, Oxley PLB. A numerical method for calculating temperature distributions in machining from force and shear angle measurements. International Journal of Machine Tool Design and Research 1976;16(4):335–49.
[32] Ernst H, Merchant ME. Chip formation, friction and high quality machined surfaces. Transactions of the American Society for Metals, Surface Treatment of Metals 1941;29:299–378.
[33] Davidson SRH, James DF. Measurement of thermal conductivity of bovine cortical bone. Medical Engineering and Physics 2000;22(10):741–7.
[34] Hoffmann KA, Chiang ST. Computational fluid dynamics for engineers. Whichita, KS: Engineering Education System; 1993.
[35] Anderson JT, Saunders OA. Convection from an isolated heated horizontal cylinder rotating about its axis. Proceedings of the Royal Society of London Series A, Mathematical, Physical & Engineering Sciences 1953;217(1131):555–62.